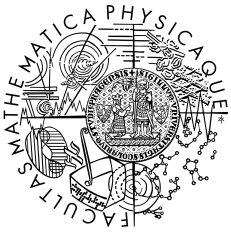

CHARLES UNIVERSITY
Faculty of mathematics
and physics

Noise and Full Counting Statistics of electronic transport through interacting nanosystems

Habilitation thesis

RNDr. Tomáš Novotný, Ph.D.

Department of Condensed Matter Physics

Prague January 2019

Acknowledgement

First, I would like to thank to Prof. Bedřich Velický for accepting me nearly 25 years ago as his (at that time) master student and later as his last Ph.D. student. Although actually none of the papers described in this thesis was done with him, only the grounds laid during my studies under his guidance enabled me to successfully follow a brand new research direction during my first postdoc stay in Copenhagen which was also arranged just due to his personal contacts with Prof. Antti-Pekka Jauho. I feel deep gratitude to him for this path.

Second, I must thank Antti for his attitude combining trust and freedom with sufficient support and control which boosted efforts of mine and my collaborators Andrea Donarini and Christian Flindt and brought us in an incredibly short time to great successes. The momentum and joy stemming from my wonderful experience in Lyngby as Antti's postdoc in 2002-4 eventually grew into a wide range of works commonly addressing the noise and full counting statistics in various nanoscopic setups presented in this habilitation thesis. Without the seed planted in Lyngby, this tree would have never brought its fruits.

Eventually, I wish to thank all of my collaborators with whom I had the pleasure to work on that decade-long journey. In particular, I am indebted to Tobias Brandes, Alessandro Braggio, Wolfgang Belzig, Federica Haupt, and Katarzyna Roszak for their invaluable contributions to our joint works. I really couldn't do all that without them.

Foreword

This habilitation thesis summarizes almost all my work devoted to the topic of electronic noise and full counting statistics (FCS) in interacting nanosystems carried out in the years 2004-2015. I started working on this topic during my first postdoc stay at DTU (Technical University of Denmark) in Lyngby (suburb of Copenhagen) with Prof. Antti-Pekka Jauho together with Antti's Ph.D. student Andrea Donarini and master student Christian Flindt. During my stay in 2002-4 I co-supervised both of them and as this research topic turned out to be quite fruitful and successful we continued our collaboration for a few more years. After my second postdoc in Copenhagen in 2004-6 at the Niels Bohr Institute with Prof. Karsten Flensberg (devoted to an unrelated topic of superconducting quantum dots), I brought the FCS topic with me back to Prague in fall 2006. It continued being my major research direction for about next 5 years, significantly fueled by a bilateral grant of the Czech Science Foundation with Prof. Tobias Brandes from TU Berlin in 2007-10 and Dr. Katarzyna Roszak taking the associated postdoc position with me in Prague. Another postdoc candidate Dr. Federica Haupt eventually chose to go to Konstanz to Prof. Wolfgang Belzig but due to Wolfgang's courtesy she could continue working on the topic of inelastic noise corrections which she started with me during her short stay in Prague in November 2007. This event seeded a whole branch of FCS research based on nonequilibrium Green's function formalism and resulted in 3 joint papers. Certain aspects of the noise topic were also subject of the master thesis of my first student Jan Prachař (defended in September 2008). I was a co-organizer, together with Tobias Brandes, of the 431. WE-Heraeus Seminar "Noise and Full Counting Statistics in Mesoscopic Transport" in May 2009 in Physikzentrum Bad Honnef, Germany. After 2011, when a new grant of the Czech Science Foundation focused on superconducting quantum dots (the second topic I imported from Copenhagen) started, the research activity on FCS has been steadily declining both on my side, since my main interest logically moved mainly to superconductivity, as well as globally — my research community of quantum transport shifted its focus to different other topics which was largely given by the lack of sufficient experimental input in the FCS subfield. For a few more years there were still papers being published, which, however, were based on results obtained by 2011. In 2013, I published an invited mini-review article in Journal of Computational Electronics (here included as P.17) which forms the basis of the present text of my habilitation thesis.

As already mentioned, I include basically all papers on the noise and FCS topic in the thesis. Altogether, it is 18 papers published between 2004 and 2015 and covering a broad scope of techniques, physical topics as well as "genres". I just left out several works published as conferences proceedings, albeit some in reasonable journals (Physics of Fluids, Physica E, J. Stat. Mech.) and with non-negligible citation numbers (e.g., J. Stat. Mech. has about 20 citations), but with subsidiary contributions from my side. On the other hand, in all the included papers I was an essential part of the research team and those papers wouldn't exist

without my major contribution. They form a wide selection of works ranging from experimental ones (P.8 and P.15) and associated theory developed just for the experiment (P.16) via technique developments (P.11 and P.12) to articles addressing purely conceptual questions (P.7 and P.10) and/or specific mechanisms (P.1, P.14, and P.18). Some of them actually bridge several of the categories and strongly reflect the nonlinear character of the highly dynamic creative processes behind their birth. Consequently, it is not easy to write a single introductory text which could exhaustively capture all their aspects in an orderly manner. To succeed at least partially I have decided to order the paper list in simple chronological order according to their publication dates. To relate individual papers to the specific parts of the introductory text, I put references to the pertinent papers in the chapter/section titles (which are reproduced in the table of contents). One should keep in mind that at least some of the papers have relation to two or even more of the sections — in such cases I have decided to mention the paper in the single section which characterizes it the best. I do hope that this approach, although imperfect, is optimal for simultaneous clarity of the introductory text and orientation in the paper list.

Contents

Chapter 1

Introduction to the FCS concept (papers P.7, P.8, and P.17)

Full Counting Statistics of electronic transport through nanoscopic systems was introduced in the 90's by papers by Levitov and Lesovik [1, 2] motivated by the photon counting statistics studied in the quantum optics for decades [3]. The quantity of interest in the FCS studies is the whole probability distribution $P_n(t)$ that n electrons passed in time t through a particular cross-section in the electronic circuit. Calculation of this probability distribution or some related (equivalent or derived) quantities such as the cumulant generating function (CGF) or individual cumulants is the core task in the field and I will review some of the methods for accomplishing this task here. The core motivation behind the FCS concept is the hope that FCS with much more information content that just the conventionally measured mean current can significantly help with the analysis of quantum transport experiments especially in the nanoscale realm (transport in quantum dots and/or molecules etc.), where the transport mechanisms are largely unknown. Thus the primary task of FCS is the *diagnostics* of nanoscopic transport mechanisms.

Even if the probability distribution $P_n(t)$ is known, one may be theoretically interested in (or the experiment only provides) various aspects of it. This is demonstrated in Fig. 1 on the elementary example of unidirectional tunneling across a high barrier (corresponding to high voltage-to-temperature ratio so that jumps back are basically impossible). Due to low transparency of the high barrier, the tunneling events are rare and uncorrelated which, analogously to the radioactive decay, corresponds to the Poissonian probability distribution of the number of passed charges $P_n(t) = (\gamma t)^n e^{-\gamma t}/n!$, $n \geq 0$ (and $P_n(t) \equiv 0$, $n < 0$) characterized by a single parameter γ giving the tunneling rate and consequently also the mean particle current. Fig. 1 depicts this simple distribution from various points of view. The first panel a) shows the Poissonian distribution for 3 different values of the mean number of passed charges $\langle n \rangle = \gamma t$. The distributions peak around the respective mean values and their width also grows in accordance with the relation $\langle\langle n^2 \rangle\rangle \equiv \langle (\Delta n)^2 \rangle = \langle n^2 \rangle - \langle n \rangle^2 = \gamma t = \langle n \rangle$ (notation: $\langle \bullet \rangle$ denotes mean values, e.g., moments of a distribution, while $\langle\langle \bullet \rangle\rangle$ are cumulants). Panel b) illustrates the very same probability distribution but now as a function of the (stochastic) particle current $I \equiv n/t$. The distributions now peak around the time-independent mean value of the current $\langle I \rangle \equiv \langle n \rangle / t = \gamma$ and with increasing time become sharper since $\langle (\Delta I)^2 \rangle = \langle (\Delta n)^2 \rangle / t^2 = \gamma / t$. Thus, the current distribution with increasing time approaches the δ-function, i.e., it is self-averaging. Panel c) offers yet an alternative point of view and exemplifies the central-limit-theorem-like behavior of $P_n(t)$. When properly scaled, the renormalized distribution $\sqrt{\gamma t} P_n(t)$ as a function

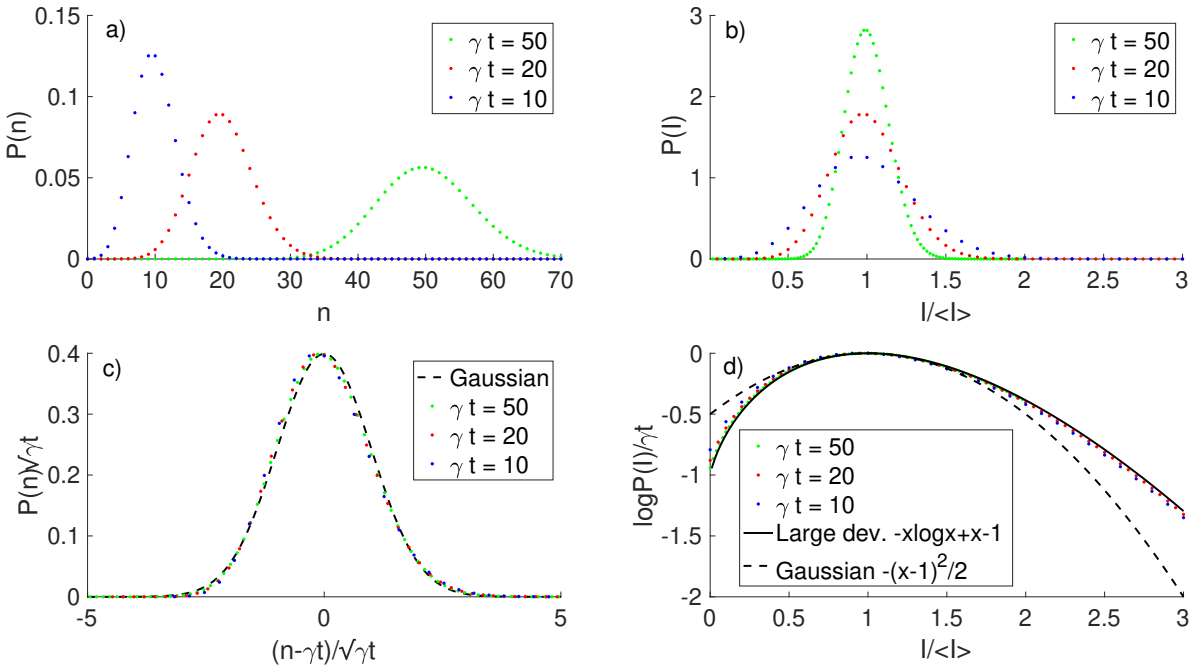

Figure 1: Full Counting Statistics of a tunnel junction. The Poissonian probability distribution of the number of passed charges $P_n(t) = (\gamma t)^n e^{-\gamma t}/n!$ is shown from various points of view. a) Plot of $P_n(t)$ for different values of parameter γt. b) Probability distribution for the particle current $I \equiv n/t$ (with the mean current $\langle I \rangle = \gamma$). c) Rescaled distribution demonstrating convergence to the Gaussian limit (dashed black line). d) Large deviation point of view, i.e., exponential resolution of the probability distribution. The Gaussian approximation of panel c) is shown again as the dashed black curve, while the large deviation result stated in the main text is the full black line nearly coinciding with the data. [Reshaped figure taken from P.17.]

of $(n-\gamma t)/\sqrt{\gamma t}$ goes to a universal Gaussian curve $e^{-x^2/2}/\sqrt{2\pi}$ (black full curve). Finally, panel d) focuses on the tails of the distribution and plots it on the logarithmic scale as a function of the current similarly to b). This is known as the *large-deviation* principle [4]. One can see again a universal result, which is, however, different from the simple Gaussian (black parabola) for currents far enough from its typical/mean value. Rather, all the distributions for various times effectively lie on the large-deviation result (dashed brown line) reading $-\iota \log \iota + \iota - 1$ with $\iota \equiv I/\langle I \rangle = n/\gamma t$, which around $\iota = 1$ coincides with the Gaussian approximation $-(\iota-1)^2/2$. These facts can be easily understood when we approximate the factorial in the Poissonian $P_n(t)$ by the Stirling formula $n! \approx (n/e)^n \sqrt{2\pi n}$ leading to $P_n(t) \approx \frac{1}{\sqrt{2\pi\gamma t \iota}} e^{-\gamma t(\iota \log \iota - \iota + 1)}$. Using $\iota \log \iota - \iota + 1 = (\iota-1)^2/2 + \mathcal{O}\left((\iota-1)^3\right)$ we get in the long-time limit the Gaussian behavior around the peak of Fig. 1c) while in the same limit we recover the large-deviation rate function [4] $R^{\text{Poisson}}(I) \equiv -\lim_{t\to\infty} \log P(t)/t = \gamma(\iota \log \iota - \iota + 1)$ in Fig. 1d).

While the self-averaging current distribution in Fig. 1b) corresponds to the most common direct measurement of the (mean) current via an ammeter, the other panels of Fig. 1 show various alternatives. It is possible to measure directly the full probability distribution $P_n(t)$ (Refs. [5, 6, 7, 8], and P.8) by a point-contact detector placed nearby the measured circuit although thus far this method is effectively limited to very weak currents in the incoherent hopping limit. Yet, good enough statistics could be obtained in P.8 to extract up to 15 cu-

mulants of the distribution. Panel c) corresponds to the situation where only the mean value and variance of the distribution is monitored. This is a compromise solution between just the mean current measurement and the full distribution function. Measuring the variance of the distribution corresponds to the zero-frequency component of the current-noise spectrum as I will show below. This is the level of characterization of nontrivial interacting quantum nanosystems currently available experimentally (Ref. [9] and P.15) which I will demonstrate on examples in Sec. 4. Panel d) shows yet a more detailed approach addressing the exponentially rare tails of the probability distribution. Experimentally, this poses the biggest challenge as the required statistics for resolving the tails of the distribution is huge. Moreover, most of the events lie in the typical window around the peak of the distribution so that only a small fraction of measured data are actually interesting. As a natural solution to this problem threshold detection schemes were proposed [10, 11] utilizing Josephson junctions (JJs) as threshold detectors. However, experiments performed so far have failed to verify the quantitative predictions even for the simplest test cases (tunnel barriers) [12, 13, 14]. It is still unclear what is behind these discrepancies, whether it is caused by the so-called environmental effects (effects of the measurement circuit) [15] or by the insufficient accuracy of theoretical predictions describing the JJ threshold detectors as discussed in P.7.

The simple tunnel junction example can be used also for the illustration of the standard probabilistic/statistical concept of the cumulant generating function (CGF). Cumulant generating function is defined as $S(\chi;t) \equiv \log \sum_{n\in\mathbb{Z}} P_n(t) e^{in\chi}$ and χ is in our context called the *counting field*.[1] The obvious basic properties of $S(\chi;t)$ are $S(\chi=0;t)=0$ from the normalization of probability and 2π-periodicity in the counting field $S(\chi+2\pi;t)=S(\chi;t)$ from the quantized discrete nature of charge $n\in\mathbb{Z}$. Its exponential (known as the characteristic function) $e^{S(\chi;t)} = \sum_n P_n(t) e^{in\chi}$ generates the moments of the probability distribution via the corresponding derivative with respect to χ at $\chi=0$, i.e., $\frac{\partial^k}{\partial(i\chi)^k} e^{S(\chi;t)}\Big|_{\chi=0} = \langle n^k\rangle(t) \equiv \sum_n n^k P_n(t)$. Moments, even though they equivalently characterize the probability distribution, have nevertheless several disadvantages: first, they are not homogeneous in t even in the large-time limit and, second, there are infinitely many of them nonzero due to the condition $\langle n^{2k}\rangle \geq \langle n^k\rangle^2$ [16].

Cumulants $\langle\langle n^k\rangle\rangle(t) \equiv \frac{\partial^k S(\chi;t)}{\partial(i\chi)^k}\Big|$, generated by the CGF being the logarithm of the moment-generating characteristic function, are proportional to t for large times (as demonstrated for the Poissonian case) and their high-order behavior is less restricted by the lower-order ones. Marcienkiewicz theorem [16] states that either only the first two cumulants are nonzero (Gaussian distribution) or all are non-zero, yet approximations truncating high-order cumulants are meaningful contrary to their counterparts for moments which necessarily break the above inequalities. Cumulants' relation to moments cannot be expressed explicitly in a simple manner — few lowest ones read $\langle\langle n\rangle\rangle = \langle n\rangle$; $\langle\langle n^2\rangle\rangle = \langle (n-\langle n\rangle)^2\rangle$; $\langle\langle n^3\rangle\rangle = \langle (n-\langle n\rangle)^3\rangle$; $\langle\langle n^4\rangle\rangle = \langle (n-\langle n\rangle)^4\rangle - 3\langle\langle n^2\rangle\rangle^2$; ... Cumulants correspond to *connected correlation functions* in the field-theoretic language and the relation between the moment-generating characteristic function and the CGF is the same as between the partition function and the thermodynamic potential (e.g., free energy). This is an important analogy which will be mentioned again in Sec. 4.2 concerning the non-equilibrium Green's functions. Questions of homogeneity in time exactly correspond to the issue of extensivity (i.e., homogeneity in volume) in the linked cluster expansion for thermodynamic potentials [17].

[1] Generally the charges can jump across a given interface in both directions and, therefore, in principle $P_n(t)$ for all integer n can be nonzero and contribute to CGF.

For the Poissonian distribution we get $S(\chi;t) = \log \sum_{n=0}^{\infty} \frac{(\gamma t)^n}{n!} e^{-\gamma t} e^{in\chi} = \gamma t(e^{i\chi} - 1)$, which is indeed homogenous in time (the *exact* proportionality to t is, however, not a generic feature). Cumulants of the Poissonian distribution are constant $\langle\langle n^k \rangle\rangle(t) = \gamma t$ and its CGF is analytic in the whole complex χ-plane, which is also a peculiarity of this particular probability distribution. It turns out that the generic behavior of CGFs is actually non-analyticity in the complex χ-plane, which implies ubiquitous factorial growth of high-order cumulants and their oscillations with parameters of the CGF, cf. P.8 and P.11, Sec. IV. I just finish this brief introduction into the properties of CGFs by pointing out the connection to the large-deviation theory of rate functions $R(I)$ determined by $P_n(t) \underset{t\to\infty}{\approx} e^{-tR(I)}$ [4]. Knowing the CGF of a distribution we can invert the relation for the characteristic function above to evaluate the $P_n(t)$ in terms of $S(\chi;t)$ as $P_n(t) = \int_0^{2\pi} \frac{d\chi}{2\pi} e^{S(\chi;t)} e^{-in\chi}$. For the Poissonian distribution we can easily calculate the integral exactly, but since I want to demonstrate a more general principle, let's consider an approximate evaluation of the integral for large t (and consequently also large n) via the steepest descent/saddle point method. The saddle point χ_0 lies on a purely imaginary axis of the complex χ-plane and satisfies the condition $\gamma e^{i\chi_0} = I$ or $i\chi_0 = \log \iota$. Consequently, $P_n(t) \underset{t\to\infty}{\approx} e^{\gamma t(e^{i\chi_0} - 1 - i\chi_0 \iota)} = e^{-tR^{\mathrm{Poisson}}(I)}$ recovering the above expression for the large-deviation rate function $R^{\mathrm{Poisson}}(I)$. However, this procedure is general and not limited to the Poissonian case only. The asymptotic large-deviation behavior of the probability distribution reads $P_n(t) \underset{t\to\infty}{\approx} e^{t(S(\chi_0;t)/t - i\chi_0 I)}$ with $\lim_{t\to\infty} \frac{1}{t} \frac{\partial S(\chi;t)}{\partial(i\chi)}\Big|_{\chi_0} = I$, i.e., the rate function $R(I)$ is the Legendre dual to the CGF normalized by (long) time and taken as a function of $i\chi$. Consequently, $R(I)$ is a convex function. Moreover, it is also positive since it determines the asymptotic behavior of bounded probability density [4].

Finally, before closing this introductory section, it should be noted that the introduced counting concept can be used in a wider context than just discrete electron counting. Analogous approach based on the evaluation of the characteristic/generating functions exists also for continuous quantities and has been applied to, e.g., the classical stochastic dynamics of superconducting phase in Josephson junctions, where it was used for calculating the (zero-frequency) voltage noise within the RSJ [18] and RCSJ [19] models, or the evaluation of quantum heat-flow distributions in electronic [20] as well as phononic [21] systems. I will demonstrate the continuous-variable counting on a coarse-grained model of electronic transport in Sec. 2.2 (corresponding to P.18).

Chapter 2

Examples of classical counting in resonant level transport

In this section I will further develop the theory of electron counting in two examples involving generic model of transport through a resonant electronic level. I assume spinless transport through a single electronic level coupled to noninteracting leads. This corresponds to realistic situations in artificial quantum dots or molecules when the spin degree of freedom is unimportant (and contributes to the transport just by the factor 2) and a single electronic level lies in the transport window of the bias voltage. This model is chosen for the simplicity and clarity of presentation of concepts and formalisms. Extension to many-level systems is straightforwardly possible. The Hamiltonian of the basic building block, i.e., the level coupled to the leads is given by

$$H_0 = \epsilon_0 d^\dagger d + \sum_{k;\alpha=L,R} \epsilon_{k\alpha} c^\dagger_{k\alpha} c_{k\alpha} + \sum_{k;\alpha=L,R} (t_{k\alpha} c^\dagger_{k\alpha} d + t^*_{k\alpha} d^\dagger c_{k\alpha}). \tag{2.1}$$

I introduce by the standard definition the tunnel couplings to the respective leads as $\gamma_\alpha(\epsilon) = 2\pi \sum_k |t_{k\alpha}|^2 \delta(\epsilon - \epsilon_{k\alpha}) \equiv \gamma_\alpha$, where I set $\hbar = 1$ (and also $e = 1$, $k_B = 1$ throughout the whole text) and assume the wide-band limit implying the energy-independence of the γ's. The two leads are separately kept in local thermodynamic equilibria at temperature T and respective chemical potentials $\mu_{L,R}$ whose difference defines the bias voltage $V \equiv \mu_L - \mu_R$. I study various examples generalizing this simple resonant level Hamiltonian by adding interaction terms potentially with other degrees of freedom (e.g., vibrations). The extra terms in the Hamiltonian are then specified at the appropriate places. Despite of quantum ingredients the electron counting considered in this chapter is still essentially classical. Truly quantum extensions with their specifics related to non-commutativity of variables will be discussed in the last chapter 4.

Apart from specifically designed experiments mentioned earlier, electrons are typically not counted directly but rather the time-dependent current is monitored and its statistics studied. The relation between the number of passed electrons $n(t)$ and current $I(t)$ is simply $n(t) = \int_0^t d\tau I(\tau)$. That implies the definition of stationary (i.e., $t \to \infty$) current cumulants reading

$$\langle\langle I^k \rangle\rangle \equiv \lim_{t\to\infty} \tfrac{\langle\langle n^k \rangle\rangle}{t} = \lim_{t\to\infty} \tfrac{d\langle\langle n^k \rangle\rangle}{dt} = k \lim_{t\to\infty} \int_0^t d\tau_{k-1} \cdots \int_0^t d\tau_1 \langle\langle I(t) I(\tau_{k-1}) \cdots I(\tau_1) \rangle\rangle, \tag{2.2}$$

which reduces to the mean stationary current $\langle\langle I \rangle\rangle = \langle I(t \to \infty) \rangle$ and zero-frequency noise

$$\langle\langle I^2 \rangle\rangle = 2 \int_0^\infty d\tau \langle \Delta I(\tau) \Delta I(0) \rangle = \int_{-\infty}^\infty d\tau \left[\langle I(\tau) I(0) \rangle - \langle I(t \to \infty) \rangle^2 \right] \tag{2.3}$$

(the mean values are evaluated with respect to the stationary state) for the first two current cumulants.

2.1 Resonant tunneling in the sequential limit

Here, I describe an archetypical example of the resonant tunneling transport through a single resonant level governed by the Hamiltonian (2.1) in the limit of small couplings γ's to the leads (compared to the temperature T or detuning of the resonant level ϵ_0 from the Fermi energies of the leads) so that the dynamics of the level occupation and charge transfer is described by a simple Markovian rate equation.[1] The dynamics of the occupation of the level $P_1(t)$ and probability of being empty $P_0(t) = 1 - P_1(t)$ satisfies the following master equation

$$\frac{d}{dt}\begin{pmatrix} P_0(t) \\ P_1(t) \end{pmatrix} = \begin{pmatrix} -\gamma_L f_L - \gamma_R f_R & \gamma_L(1-f_L) + \gamma_R(1-f_R) \\ \gamma_L f_L + \gamma_R f_R & -\gamma_L(1-f_L) - \gamma_R(1-f_R) \end{pmatrix} \cdot \begin{pmatrix} P_0(t) \\ P_1(t) \end{pmatrix}, \tag{2.4}$$

where $f_{L/R} \equiv \left(e^{(\epsilon_0 - \mu_{L/R})/T} + 1\right)^{-1}$ are the Fermi-Dirac distributions of the respective leads at the resonant-level energy. By the identification of the various Fermi-golden-rule rates with corresponding charge-transfer processes (e.g., $\gamma_L f_L$ corresponds to the transfer of charge from the left lead onto the resonant level, while $\gamma_L(1-f_L)$ describes the reverse process etc.) we can straightforwardly extend the master equation to include the charge counting say across the left tunneling barrier and write the pertinent master equation for the *joint* probability distribution $P_{0/1}(n;t)$ of level being empty/occupied and n charges having passed through the left tunnel barrier (the positive direction is chosen to be from the left lead towards the resonant level)

$$\frac{dP_0(n;t)}{dt} = -(\gamma_L f_L + \gamma_R f_R)P_0(n;t) + \gamma_L(1-f_L)P_1(n+1;t) + \gamma_R(1-f_R)P_1(n;t), \tag{2.5a}$$

$$\frac{dP_1(n;t)}{dt} = \gamma_L f_L P_0(n-1;t) + \gamma_R f_R P_0(n;t) - [\gamma_L(1-f_L) + \gamma_R(1-f_R)]P_1(n;t). \tag{2.5b}$$

Introducing $\tilde{P}_{0/1}(\chi;t) = \sum_n P_{0/1}(n;t)e^{in\chi}$ we have

$$\frac{d}{dt}\begin{pmatrix} \tilde{P}_0(\chi;t) \\ \tilde{P}_1(\chi;t) \end{pmatrix} = \begin{pmatrix} -\gamma_L f_L - \gamma_R f_R & \gamma_L(1-f_L)e^{-i\chi} + \gamma_R(1-f_R) \\ \gamma_L f_L e^{i\chi} + \gamma_R f_R & -\gamma_L(1-f_L) - \gamma_R(1-f_R) \end{pmatrix} \cdot \begin{pmatrix} \tilde{P}_0(\chi;t) \\ \tilde{P}_1(\chi;t) \end{pmatrix} \equiv \mathbf{W}(\chi)\cdot\tilde{\mathbf{P}}(\chi;t) \tag{2.6}$$

with the solution $\tilde{\mathbf{P}}(\chi;t) = \exp(\mathbf{W}(\chi)t)\cdot\tilde{\mathbf{P}}_{\text{init}}(\chi;t=0)$. We are interested in the CGF for long times which approaches $\lim_{t\to\infty} S(\chi;t)/t = \lambda_0(\chi)$ ([22] and P.3), where $\lambda_0(\chi)$ is the eigenvalue of the generalized rate matrix $\mathbf{W}(\chi)$ with the largest real part. For small χ's relevant for the evaluation of the cumulants (derivatives of CGF at $\chi = 0$) eigenvalue $\lambda_0(\chi)$ is the one adiabatically developed from the zero eigenvalue corresponding to the stationary state of the level at $\chi = 0$. For arbitrary χ other branches of the characteristic solution might be relevant with interesting topological properties [23]. Here, let's only consider the small-χ branch with

$$\lambda_0(\chi) = \frac{\gamma_L + \gamma_R}{2}\left(\sqrt{1 + \frac{4\gamma_L\gamma_R}{(\gamma_L+\gamma_R)^2}\left[f_L(1-f_R)\left(e^{i\chi}-1\right) + f_R(1-f_L)\left(e^{-i\chi}-1\right)\right]} - 1\right). \tag{2.7a}$$

[1] The full solution of the model (2.1) is discussed in Sec. 4.2.

The first two current cumulants, i.e., the mean current and the zero-frequency noise, are

$$\langle I\rangle = -i\lambda_0'(0) = \frac{\gamma_L\gamma_R\,(f_L - f_R)}{\gamma_L+\gamma_R} \tag{2.7b}$$

and

$$\langle\langle I^2\rangle\rangle = -\lambda_0''(0) = \frac{\gamma_L\gamma_R}{\gamma_L+\gamma_R}\cdot\frac{(\gamma_L^2+\gamma_R^2)\,(f_L+f_R-2f_Lf_R)+2\gamma_L\gamma_R\,[f_L(1-f_L)+f_R(1-f_R)]}{(\gamma_L+\gamma_R)^{\,2}}. \tag{2.7c}$$

Two limits are instructive to consider:

1. Zero bias voltage $V\to 0$ (equilibrium case, $f_L = f_R = f$). Current is zero while the thermal noise remains finite $\langle\langle I^2\rangle\rangle \underset{V\to 0}{=} 2f(1-f)\frac{\gamma_L\gamma_R}{\gamma_L+\gamma_R}$ and can be related via the equilibrium *fluctuation-dissipation theorem* $\langle\langle I^2\rangle\rangle_{V\to 0} = 2TG$ to the linear conductance $G = \frac{\partial\langle I\rangle}{\partial V}\Big|_{V\to 0} = -f'\frac{\gamma_L\gamma_R}{\gamma_L+\gamma_R}$. Notice that the CGF (2.7a) is not just a quadratic function of the counting field χ even in equilibrium, i.e., the thermal equilibrium fluctuations of a nanoscopic system are not Gaussian but contain also higher-order (even) cumulants (equilibrium CGF is an even function of χ).

2. Large symmetrically applied bias voltage so that $f_L\to 1$, $f_R\to 0$ (shot noise limit). Current $\langle I\rangle = \frac{\gamma_L\gamma_R}{\gamma_L+\gamma_R}$ and noise expressed in terms of the *Fano factor* $F = \langle\langle I^2\rangle\rangle/\langle I\rangle = \frac{\gamma_L^2+\gamma_R^2}{(\gamma_L+\gamma_R)^2}$ are given by the well-known formulas [24]. Fano factor lies between 1/2 for a symmetric double-barrier structure $\gamma_L = \gamma_R$ and the Poissonian value 1 for a very asymmetric one, say $\gamma_L \gg \gamma_R$ (effectively, the transport is fully determined and limited by just the right barrier and the FCS approaches the Poissonian case considered in the introductory chapter 1). CGF in this shot-noise limit reads

$$\lambda_0(\chi) \underset{V\to\infty}{=} \frac{\gamma_L+\gamma_R}{2}\left(\sqrt{1+\frac{4\gamma_L\gamma_R\,(e^{i\chi}-1)}{(\gamma_L+\gamma_R)^2}}-1\right) \tag{2.8}$$

and exhibits the generic (square-root) singularities in the complex χ-plane leading to the universal factorial growth and oscillations of high-order cumulants (P.8 and [25]) as well as the seeming breaking of 2π-periodicity in χ for the symmetric case $\gamma_L = \gamma_R$ related to the topological phase transitions in the generalized-rate-matrix spectrum [23].

This example, however simple, illustrates the general method used for the evaluation of the FCS for nanostructures with many levels and arbitrary number of leads in the incoherent tunneling regime, which typically involves Coulomb blockade [22], described by master equations for many-body-level occupations. The prescription for the construction of the generalized rate matrix of Ref. [22] via the inclusion of the counting field(s) is just a straightforward extension of the approach used in this example. The CGF for current statistics is then just the appropriate eigenvalue of the generalized rate matrix[2]. Moreover, the charge conservation can be generally

[2]For larger systems it is not possible any longer to express the eigenvalue analytically like here in Eq. (2.7a). Yet, one can still find the cumulants semi-analytically using the recurrent scheme of P.6 briefly introduced in Sec. 4.1.

proven from the structure of the generalized rate matrix ([22] and P.2). For the present two-lead setup, this means that the CGFs evaluated with counting fields either at the left or right junctions are identical (provided the positive directions of current were chosen consistently) yielding the same current cumulants at the two junctions. This expresses the charge conservation in the stationary regime, when mean current, zero-frequency noise, etc. do not depend on the cross-section along the circuit where they are measured.

2.2 Inelastic corrections to resonant transport in the large-voltage regime (paper P.18)

In this section, I study a less-trivial example of classical counting of electrons. Once again, we consider transport across a resonant level (2.1) which is now weakly coupled to an otherwise isolated local vibrational mode with the frequency ω and free linear-harmonic-oscillator Hamiltonian $H_{\rm vib} = \omega a^\dagger a$ via the interaction Hamiltonian $H_{\rm int} = Md^\dagger d(a+a^\dagger) = \sqrt{2}Md^\dagger dQ$ coupling the level occupation $d^\dagger d$ to the displacement of the local oscillator $Q = (a + a^\dagger)/\sqrt{2}$. Even in the weak coupling regime evaluation of the FCS is a challenging quantum problem, which will be discussed in the quantum regime later in Sec. 4.2, but it has a simple physically intuitive solution in the limit of large bias [P.18]. For simplicity we assume that the symmetric coherent coupling $\gamma = \gamma_L + \gamma_R \equiv 2\gamma_L$ is the largest energy scale of the problem, in particular it is much larger than the symmetrically applied bias voltage V which, in turn, is bigger than the vibration frequency and temperature $\gamma \gg V \gg \omega, T$ (recall the convention $e = \hbar = k_B = 1$). The elastic transport is governed by the transmission coefficient $\mathcal{T} = \frac{\gamma^2}{\Delta^2+\gamma^2}$ with $\Delta = \epsilon_0 - \mu$ being the offset of the resonant level from the equilibrium chemical potential of the leads ($\mu_{L,R} = \mu \pm V/2$). In the large-voltage limit $V \gg \omega$ the characteristic time of electron tunneling across the nanosystem $1/V$ is much shorter than the period of oscillation $2\pi/\omega$ of the vibrational mode and, thus, the oscillator may be considered as adiabatically gating the single electronic level and consequently changing the electronic transmission coefficient $\mathcal{T}(Q) = \frac{\gamma^2}{(\Delta-\sqrt{2}MQ)^2+\gamma^2}$. The mean current then results from the averaging the oscillator position $Q(t) = A\cos\omega t$ over the oscillation period $2\pi/\omega$. The first nonzero correction stems from the second order in M expansion of the expression for $\langle\mathcal{T}(Q)\rangle \approx \mathcal{T} + 2(M^2\mathcal{T}^2/\gamma^2)(3-4\mathcal{T})\langle Q^2\rangle$. Performing the average one gets $\langle Q^2\rangle = A^2/2 = \overline{N} + 1/2$ with $\overline{N}$ the mean occupation number of the oscillator. This yields the mean inelastic correction to the current $\overline{I}_{\rm inel} = (\langle\mathcal{T}(Q)\rangle - \mathcal{T})\,V = I_0(\overline{N} + 1/2)$ with $I_0 = 2VM^2\mathcal{T}^2(3-4\mathcal{T})/\gamma^2$ [P.9]. We can extend this result by considering slow fluctuations of the oscillator amplitude $A(t)$ or, equivalently, the oscillator occupation number $N(t)$ driven by the fluctuating energy exchange between the oscillator and the passing electrons on a timescale much longer than the oscillator period $2\pi/\omega$. This timescale is governed by the inverse of the rates $\alpha_{\downarrow,\uparrow}$ for increasing/decreasing the oscillator occupation number entering the birth-death type of master equation for the occupation number probability density $p_k(t)$ that $N(t) = k$ ([26, 16, 27] and P.13)

$$\frac{dp_k(t)}{dt} = \alpha_\downarrow\big[(k+1)p_{k+1}(t) - kp_k(t)\big] + \alpha_\uparrow\big[kp_{k-1}(t) - (k+1)p_k(t)\big]. \tag{2.9}$$

Nonequilibrium rates $\alpha_{\downarrow,\uparrow}$ can be evaluated microscopically ([28, 29] and P.13) and are proportional to $\omega M^2\mathcal{T}^2/\gamma^2$ with the small dimensionless coupling constant $M^2\mathcal{T}^2/\gamma^2 \ll 1$ ensuring the required time-scale separation. Under these conditions we have $I_{\rm inel}(t) = I_0 N(t)$ for the

inelastic current correction (more precisely, its dynamical part, i.e., without the constant factor $I_0/2$ contributing solely to the mean current). The passed charge used in the FCS now reads $Q_{\mathrm{inel}}(t) \equiv \int_0^t d\tau I_{\mathrm{inel}}(\tau) = I_0 \int_0^t d\tau N(\tau)$. Obviously, in this coarse-graining approach the charge is no longer discrete and rather $Q_{\mathrm{inel}}(t)$ is a continuous random variable which is a simple functional of the stochastic process $N(t)$. Analogously to the previous subsection we can write again an extended master equation for the *joint* probability density $p_k(q,t)$ of the state of the system (oscillator occupation $N(t) = k$) *and* the number of passed charges $Q(t) = q$

$$\frac{\partial p_k(q,t)}{\partial t} = \alpha_\downarrow\big[(k+1)p_{k+1}(q,t) - kp_k(q,t)\big] + \alpha_\uparrow\big[kp_{k-1}(q,t) - (k+1)p_k(q,t)\big] - I_0 k\frac{\partial p_k(q,t)}{\partial q}. \tag{2.10}$$

This equation can be recast into an equivalent form for the Laplace-transformed quantity $\tilde{p}_k(\chi,t) \equiv \int_{-\infty}^{\infty} dq e^{i\chi q} p_k(q,t)$ more suitable for the direct evaluation of the cumulant generating function (CGF) $S(\chi;t) = \log \sum_{k=0}^{\infty} \tilde{p}_k(\chi,t)$ via

$$\frac{\partial \tilde{p}_k(\chi,t)}{\partial t} = \alpha_\downarrow\big[(k+1)\tilde{p}_{k+1}(\chi,t) - k\tilde{p}_k(\chi,t)\big] + \alpha_\uparrow\big[k\tilde{p}_{k-1}(\chi,t) - (k+1)\tilde{p}_k(\chi,t)\big] + i\chi I_0 k\tilde{p}_k(\chi,t). \tag{2.11}$$

This equation can be solved by the method of characteristics [27, Sec. VI.6.] and the final result reads (details can be found in P.18)

$$\lim_{t\to\infty} \frac{S(\chi;t)}{t} = \frac{\alpha_\downarrow - \alpha_\uparrow - i\chi I_0 - \sqrt{(\alpha_\downarrow + \alpha_\uparrow - i\chi I_0)^2 - 4\alpha_\downarrow\alpha_\uparrow}}{2}. \tag{2.12}$$

Since the charge in our approximation is not quantized, the resulting CGF is not 2π-periodic in the counting field χ. Nevertheless, CGF still possesses the generic branch-cuts in the complex χ-plane repeatedly mentioned previously. This CGF is identical in the large-voltage limit to the one calculated fully microscopically with significantly bigger computational effort [30] and it generates the nonequilibrium inelastic corrections to the mean current and noise consistent with previous studies [P.9, P.13]. Large voltage behavior of cumulants $\langle\langle I^m \rangle\rangle \propto V^{2m}$ stemming from (2.12) which agrees with the corresponding quantum result by Utsumi et al. [30] is at variance with earlier results by Urban et al. [31] predicting $\langle\langle I^m \rangle\rangle \propto V^{m+1}$. Although the exact source of discrepancy of the two microscopic approaches is not fully identified yet, our physically intuitive classical calculation presented here has convinced even the authors of Ref. [31] that their method must be incorrect.

Chapter 3

Counting at interfaces described by the quasi-classical singular coupling limit (papers P.1–P.5 and P.10)

It was in this specific quasi-classical limit where I first encountered the counting concept as an active part of my research. It was connected with the study of quantum dynamics of so called nanoelectromechanical systems (NEMSs), in particular the "quantum shuttle" [32] with the setup schematically shown in Fig. 2. Due to their potentially strong coupling to the leads such NEMSs are typically described by the generalized master equation (GME) in a special form which is known in mathematical physics context under the name of *singular coupling limit* [33]. In electronic transport this approximation can be justified in the limit of energy-independent tunnel coupling between the system and leads (so called wide-band limit) and large bias voltage effectively keeping one of the leads occupied at any energy while the other one is always empty [34, 35] (see the scheme in Fig. 2). The advantage of this approximation is that the electron hopping between the leads and the system is described locally, only by system operators living at the interface. This is very different even from the standard weak coupling approach, where the coupling is determined from the eigenstates of the system Hamiltonian and, consequently, is typically highly nonlocal throughout the whole system/device. The hopping superoperator entering the singular-coupling GME can be easily identified solely from the tunneling part of the total Hamiltonian and the immediate hopping interpretation of the resulting term leads to

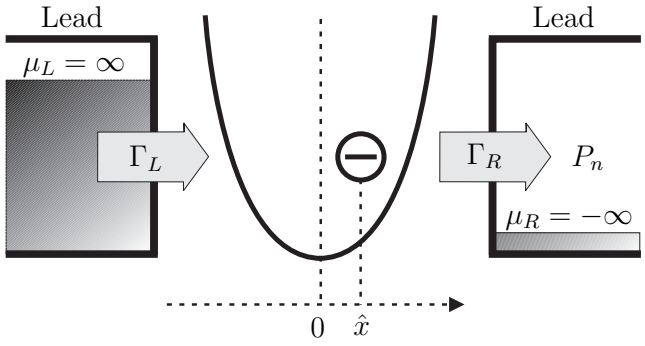

Figure 2: The quantum shuttle consists of a nanosized grain moving in a harmonic potential between two leads. A high bias between the leads drives electrons through the grain. [Figure taken from P.3.]

a simple counting picture at the interface. In more detail, the GME has this generic form

$$\dot{\hat{\rho}}^{(n)}(t) = (\mathcal{L} - \mathcal{I})\hat{\rho}^{(n)}(t) + \mathcal{I}\hat{\rho}^{(n-1)}(t) \ , \tag{3.1}$$

with $n = 0, 1, \ldots$ and $\hat{\rho}^{(-1)}(t) \equiv 0$. From the n-resolved density operator one can obtain, at least in principle, the complete probability distribution $P_n(t) = \mathrm{Tr}\left[\hat{\rho}^{(n)}(t)\right]$ which can then be used for the evaluation of the FCS exactly as in previous sections. It can be also used for the evaluation of the finite-frequency current noise spectrum $S_I(\omega)$, which was also considered in the works P.4 and P.6, via the so-called MacDonald formula [36, 37] reading

$$S_I(\omega) = \omega \int_0^\infty dt \sin(\omega t) \frac{d}{dt}\Big[\sum_n n^2 P_n(t) - \big(\sum_n n P_n(t)\big)^2\Big] \ . \tag{3.2}$$

It should be noted, however, that despite of the simple quasi-classical interpretation of the electron hopping process at the interface(s), the system Liouvillean $\mathcal{L}$ as well as the hopping/current superoperator $\mathcal{I}$ in principle capture fully quantum internal dynamics of the system under consideration including various interference phenomena and coherence effects. It is just the instant electron hopping at the interface(s) enabling simple quasi-classical counting simplifying the whole approach in the given limit, but the internal dynamics of the system can be arbitrarily complicated and deeply in the quantum regime (which can be the case in double- and/or triple-dot setups considered in P.10 and P.2).

Having found the explicit form for the superoperators $\mathcal{L}$ and $\mathcal{I}$ for a given problem (e.g., the single-dot quantum shuttle), the zero- and/or finite-frequency noise can be evaluated by using an operator generalization of the generating function method as in P.1, P.2 and/or P.4.[1] Another possibility is the perturbative evaluation of the cumulant generating function (corresponding to the extremal eigenvalue of a modified Liouvillean analogously to (2.7a) in Sec. 2.1) as was done up to the third cumulant in P.3 (the perturbative method was significantly extended in P.6 and I correspondingly discuss it more explicitly in the following chapter). In any case, the resulting formulae involve two basic quantities which typically must be calculated numerically: the stationary density matrix $\hat{\rho}^{\mathrm{stat}}$ determined as the null vector of the Liouvillean $\mathcal{L}\hat{\rho}^{\mathrm{stat}} = 0$ and a pseudoinverse of the Liouvillean $\mathcal{R}$ (i.e., inverse of $\mathcal{L}$ taken solely on the complement of the null space). These quantities can be numerically hard to obtain — for example for the single-dot shuttle they involved superoperator matrices with linear size 20 000 which were 15 years ago at the edge of (especially internal memory) capacity of usual PCs. The direct evaluation was really impractical also because of long computational times so that we developed with substantial help of numerical mathematician Prof. Timo Eirola from Helsinki University of Technology (now renamed the Aalto University) Arnoldi iterative schemes for the computation of $\hat{\rho}^{\mathrm{stat}}$ and $\mathcal{R}$ (applied to a given vector). Since $\mathcal{L}$ is not hermitian, we couldn't use the more standard Lanczos algorithm. To achieve convergence of the Arnoldi iteration we had to develop a preconditioner, which corresponded to the solution of the Sylvester part of the problem, cf. Appendix A of P.2.

Alternatively, in some setups involving internal charge flows within the system (such as double-dot of P.10 or triple-dot in P.2) the zero-frequency current noise can be equivalently calculated using these internal current operators with the help of the *quantum regression theorem* [26]. Charge conservation implies exactly that all current cumulants must be constant

[1] Finite-frequency noise spectrum is *not* constant along the circuit, unlike its zero-frequency counterpart, and, thus, it's evaluation requires more detailed information about the junction such as relative capacitances between the system and the two leads as explained in P.4.

along the circuit, i.e., it doesn't matter at which position the current is evaluated (this issue is explained in detail in Sec. III of P.2). However, the exact identities stemming from the charge conservation may be broken by adopted approximations and this is indeed the case in the model of a dissipative double-quantum-dot studied in P.10. There we showed with my master student Jan Prachař that various commonly used approximations in a GME equation describing joint effects of electronic leads and dissipative bosonic bath on a double-dot lead to significant issues in the resulting noise. These noise issues are a specific manifestation of generic problems of Markovian GMEs [26, 38] and of general non-additivity of multiple baths (which we discussed briefly already in Sec. II.B of P.2 and which still forms an active research topic as seen, e.g., in Ref. [39]). There seems to be no satisfactory universal solution of such problems within the framework of Markovian GMEs, but there are no generic viable non-Markovian extensions available either. The only reliable solution of such problems can be probably achieved just by heavy numerical tools such as Quantum Monte Carlo recently developed for the FCS of nonequilibrium single-impurity Anderson model [40]; in our group this numerical methodology is pursued by my former postdoc Martin Žonda and, once its implementation is completed, it may serve as an invaluable benchmark of far simpler (semi)analytical methods.

Finally, I devote the rest of this chapter to a brief introduction to a prime example of FCS usage in its original spirit as a diagnostic tool of a nontrivial quantum transport mechanism. For that we look at the single-dot quantum shuttle of Fig. 2 again. In our first paper addressing this system [32] we concluded from the stationary Wigner function that in an intermediate mechanical damping regime the transport through the movable quantum dot happens via some form of coexistence of (essentially static) tunneling and shuttling mechanisms. The exact dynamical picture of this coexistence was unclear and missing. When studying the electronic noise in this model in P.1, we noticed a huge enhancement of noise quantified by the Fano factor reaching values of several hundreds. Based on this result we conjectured that the coexistence is actually a bistable switching between the two dynamical mechanisms with timescale(s) much longer than the typical transport times of individual electrons. To verify this assumption we calculated numerically also the third cumulant in P.3 and compared it with the expected analytical results for dynamically bistable systems.

FCS of such bistable systems has been studied [41], and it was found that the first three cumulants are (assuming that the individual channels are noiseless, which is a fair approximation in the shuttle case)

$$\langle\langle I \rangle\rangle = \frac{I_{\mathrm{S}}\Gamma_{\mathrm{S}\leftarrow\mathrm{T}} + I_{\mathrm{T}}\Gamma_{\mathrm{T}\leftarrow\mathrm{S}}}{\Gamma_{\mathrm{T}\leftarrow\mathrm{S}} + \Gamma_{\mathrm{S}\leftarrow\mathrm{T}}} \,, \tag{3.3a}$$

$$\langle\langle I^2 \rangle\rangle = 2(I_{\mathrm{S}} - I_{\mathrm{T}})^2 \frac{\Gamma_{\mathrm{S}\leftarrow\mathrm{T}}\Gamma_{\mathrm{T}\leftarrow\mathrm{S}}}{(\Gamma_{\mathrm{S}\leftarrow\mathrm{T}} + \Gamma_{\mathrm{T}\leftarrow\mathrm{S}})^3} \,, \tag{3.3b}$$

$$\langle\langle I^3 \rangle\rangle = 6(I_{\mathrm{S}} - I_{\mathrm{T}})^3 \frac{\Gamma_{\mathrm{S}\leftarrow\mathrm{T}}\Gamma_{\mathrm{T}\leftarrow\mathrm{S}}(\Gamma_{\mathrm{T}\leftarrow\mathrm{S}} - \Gamma_{\mathrm{S}\leftarrow\mathrm{T}})}{(\Gamma_{\mathrm{S}\leftarrow\mathrm{T}} + \Gamma_{\mathrm{T}\leftarrow\mathrm{S}})^5} \,. \tag{3.3c}$$

Here $I_{\mathrm{S/T}}$ denote the current associated with the shuttling/tunneling channel (these are known even analytically), while $\Gamma_{\mathrm{T}\leftarrow\mathrm{S}}$ is the transition rate from the shuttling to the tunneling channel and $\Gamma_{\mathrm{S}\leftarrow\mathrm{T}}$ is the rate of the reverse transition. Their calculation is a highly nontrivial and technically demanding task as is demonstrated in P.5, Sec. 5.3 in a special limit for the single-dot quantum shuttle. FCS offers an elegant alternative utilizing its diagnostic power — as we showed in P.3 by calculating numerically the first three cumulants of the current, i.e., the mean current, zero-frequency noise, and the third cumulant called "skewness", we can extract the two switching rates from the first two cumulants (mean current and noise) using formulas (3.3a) and

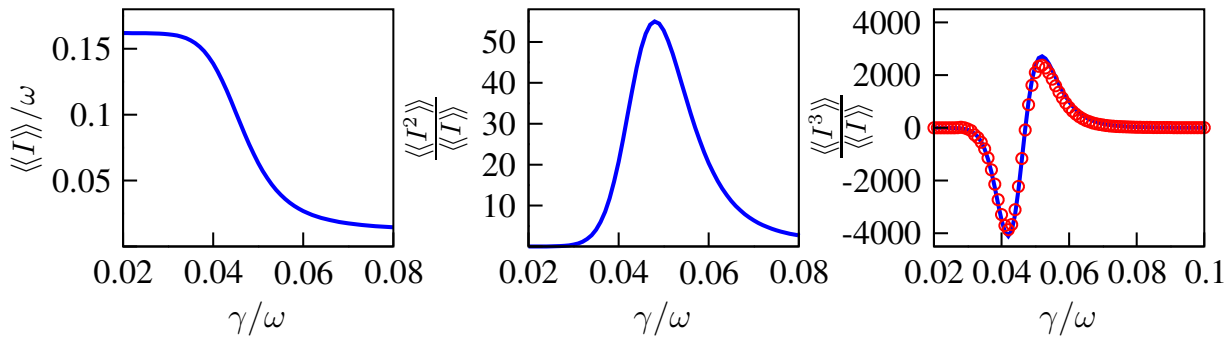

Figure 3: Results for the first three cumulants in the quantum shuttle as functions of its mechanical damping γ. The full lines indicate numerical results, while the circles in the rightmost panel are given by the analytic expression (3.3c) for the third cumulant assuming that the shuttle in the transition region effectively behaves as a bistable system. [Figure taken from P.3.]

(3.3b) for the dichotomous process and then (successfully) test the bistability assumption by plugging these rates in to the analytical formula (3.3c) for the third cumulant of the dichotomous process and comparing it to the full numerical solution (cf. Fig. 3).

We used a similar methodology with my postdoc Martin Žonda in a different context of purely classical stochastic dynamics of underdamped Josephson junctions (so called RCSJ model) [19] to decipher various dynamical regimes of the noisy phase evolution and obtained highly nontrivial quantitative results for the switching rates between trapped and running solutions as well as rates of multiple phase slips. Also there the counting field approach proved its extreme usefulness as a diagnostic tool enabling unambiguous identification and quantitative characterization of dynamics of nanoscopic systems.

Chapter 4

Counting in the fully quantum regime

Counting electrons in the quantum regime, i.e., when quantum-mechanical coherent effects are relevant, is intimately related to the issues of quantum measurement and detection schemes analogously to the situation in quantum optics. The conceptual problems are particularly obvious when there is explicit coherence between the two parts of the circuit divided by the cross-section, where the counting is supposed to take place in a "gedanken experiment". This is realized for example in Josephson junctions with flowing supercurrent driven by phase difference [42], but formulation problems exist similarly in the normal case as well. Strong projective measurement can be applied to strictly monitor charge transfers such as in the experiments involving the quantum point contact in close proximity of the studied system ([5, 6, 7, 8] and P.8) which, however, completely kills the quantum coherence and renders the transport essentially classical. An alternative is to weakly couple a current detector so as to perturb the studied system the least possible. One should then study the full quantum-mechanical dynamics of the system + detector. The issues of the detector back-action are beyond the scope of this work, I refer readers to the proceedings [43] and references therein.

When the dynamics and thus also the backaction of the detector is neglected ("virtual detector"), one can formulate a quantum-mechanical formula for the CGF in the quantum regime [44, 45]

$$e^{S(\chi;t)} = \left\langle T_C \exp\left[-\frac{i}{2}\int_C d\tau \chi(\tau) I(\tau)\right]\right\rangle \tag{4.1}$$

formulated as a generating functional on the Keldysh contour C. The counting field $\chi(\tau)$ assumes for long times t opposite constant values $\pm\chi$ on the two branches of the Keldysh contour and couples to the measured current through the circuit represented by the current operator $I(\tau)$ in the interaction picture with respect to the system Hamiltonian. The mean value is taken with respect to the nonequilibrium state of the electronic system. This effectively describes the influence functional due to the electronic circuit on the quantum coordinate (antisymmetric on the Keldysh contour) of the detector. For the current operator localized at either of the tunnel junctions ($\alpha = L$, R) the coupling term $\chi_\alpha(\tau) I_\alpha(\tau)$ can be moved by a gauge transformation into the respective tunneling term of the Hamiltonian by modifying

$$\begin{aligned} H_{T\alpha} &= \sum_k (t_{k\alpha} c_{k\alpha}^\dagger d + t_{k\alpha}^* d^\dagger c_{k\alpha}) \longmapsto \\ H_{T\alpha}(\chi_\alpha(\tau)) &= \sum_k \left(t_{k\alpha} c_{k\alpha}^\dagger d e^{i\chi_\alpha(\tau)/2} + t_{k\alpha}^* d^\dagger c_{k\alpha} e^{-i\chi_\alpha(\tau)/2} \right). \end{aligned} \tag{4.2}$$

This contour-dependent modification of the system Hamiltonian is the starting point for the

evaluation of the CGF in the quantum case. The appropriate derivatives of the CGF yield for large times the current cumulants with Keldysh ordering. In particular, the first cumulant simply gives the quantum-mechanical mean value of the current, while the second one yields the zero-frequency component of the symmetrized irreducible current-current correlation function, i.e., the noise.

It should be noted that the probabilities $P_n(t) = \int_0^{2\pi} \frac{d\chi}{2\pi} e^{S(\chi;t)} e^{-in\chi}$ calculated from Eq. (4.1) are generally not positive, in particular for superconducting transport [42]. This can be understood by realizing the origin of formula (4.1) as stemming from the description of the measurement scheme. In the superconducting case the current depends on the superconducting phase difference which is a conjugated variable to the number of passed charges. The attempts of their simultaneous measurement necessarily cause problems reflected in "negative probabilities". Instead of interpreting P_n's as probabilities, it is more sensible to relate them to the Wigner function of the measurement apparatus which can turn negative [42].[1]

4.1 Generalized Master Equation approach: quantum memory effects at resonant Fermi edges (papers P.6, P.11, P.14, P.15, and P.16)

The above modified Hamiltonian (4.2) can be used also in approaches involving the reduced density matrix of the nanosystem. The starting Liouville-von Neumann equation for the whole generalized density matrix $\tilde{\varrho}(\chi;t)$ of the system + reservoirs (leads) then gets modified into [47, 48]

$$i\frac{d\tilde{\varrho}(\chi;t)}{dt} = H(\chi)\tilde{\varrho}(\chi;t) - \tilde{\varrho}(\chi;t)H(-\chi). \tag{4.3}$$

This requires the appropriate modification of the standard methods for the evaluation of reduced density matrix $\tilde{\rho}(\chi;t) = \mathrm{Tr}_{\mathrm{res}}\tilde{\varrho}(\chi;t)$ of the system only. It can be easily shown that within the lowest-order approximation, i.e., the second order in the tunnel couplings $t_{k\alpha}$ corresponding to the Fermi-golden-rule rates the master equation resulting from the Liouville-von Neumann equation with counting field(s) is identical to that of Sec. 2.1 and prescription of Bagrets and Nazarov [22]. Going beyond the lowest-order approximation requires more sophisticated approaches as non-classical effects such as cotunneling, level broadening, and/or (quantum) memory become important. Standard GME approaches capable of including these effects were extended to incorporate the counting field(s). The first study [48] used the perturbative real-time diagrammatic technique [49, 50] to go beyond the lowest-order tunneling limit by incorporating the next order (cotunneling) with ensuing non-Markovian effects revealed by noise and higher-order cumulants. Infinite resummation of the perturbative series within the so-called resonant tunneling approximation [49, 51] was performed in Refs. P.14 and [52]. It was concluded that repeating the successful approximation scheme with the counting field does not necessarily reproduce the properties of the results without the counting field (i.e., results for the mean current only) such as the exactness for noninteracting systems [P.14]. At the level of noise and higher cumulants there are omitted diagrams even in the noninteracting case [52], yet the approximation scheme still generally performs better than less sophisticated ones. Nevertheless, development of reliable approximations for resummation of perturbation series for GMEs remains an open issue.

[1] A fresher point of view based on non-classical dynamics can be found in more recent Ref. [46].

We have developed for general non-Markovian GMEs a recurrent evaluation method of high-order cumulants based on a perturbative expansion of the extremal eigenvalue of the generalized (by inclusion of the counting field(s)) memory kernel [P.6]. The recurrent scheme is very stable and enables to reach high-order cumulants (order of tens) well in the regime of universal oscillations P.11. Here, I will use it just to calculate the second cumulant (i.e., noise) for a fundamentally non-Markovian problem of low-temperature transport close to Fermi edges [P.15, P.16]. I start with showing the principle of the recurrent scheme on the problem of noise evaluation for a general non-Markovian generalized memory kernel. Higher-order cumulants are obtained by following the recurrent scheme further on.

Let's consider a GME for the generalized reduced density matrix $\tilde{\rho}(\chi;t)$ in the general form [P.6]

$$\frac{d\tilde{\rho}(\chi;t)}{dt} = \int_0^t dt' w(\chi;t-t')\tilde{\rho}(\chi;t') + \eta(\chi;t). \tag{4.4}$$

The CGF is then given as $S(\chi;t) = \log \mathrm{Tr}_{\mathrm{sys}}\tilde{\rho}(\chi;t)$ which for the long times $t \to \infty$ is determined[2] by the pole $z_0(\chi)$ of the resolvent $[z - \mathcal{W}(\chi;z)]^{-1}$ of the Laplace-transformed version of Eq. (4.4) (P.6 and P.11) with $\mathcal{W}(\chi;z) \equiv \int_0^\infty dt e^{-zt} w(\chi;t)$. This pole yielding the CGF $\lim_{t\to\infty} S(\chi;t)/t = z_0(\chi)$ is the solution of the equation

$$z_0(\chi) = \lambda_0(\chi; z_0(\chi)) \tag{4.5}$$

with $\lambda_0(\chi;z)$ the extremal eigenvalue of $\mathcal{W}(\chi;z)$ adiabatically developed for small χ from zero corresponding to the stationary state (without the counting field). Since cumulants are determined by the Taylor expansion of $S(\chi;t)$ around $\chi = 0$ we can determine the eigenvalue $\lambda_0(\chi;z)$ perturbatively via the Rayleigh-Schrödinger perturbation scheme. Then also the equation for the pole $z_0(\chi)$ (4.5) can be solved perturbatively in χ which completes the task of cumulant evaluation.

The full recurrent procedure is explained in detail in P.6 and P.11, here I only demonstrate it on the evaluation of the mean current and noise. Because of the probability conservation condition $\mathrm{Tr}_{\mathrm{sys}}\tilde{\rho}(\chi=0;t) = 1$ for any t which implies for the kernel $\mathrm{Tr}_{\mathrm{sys}}\mathcal{W}(\chi=0;z)\bullet = 0$ for any z and, consequently, also $\lambda_0(\chi=0;z) = 0$, we can write for the eigenvalue up to the second order in χ and z: $\lambda_0^{(2)}(\chi;z) = \lambda_0'\chi + \lambda_0''\chi^2/2 + \dot{\lambda}_0'\chi z$. Then, we can solve Eq. (4.5) up to the second order in χ as $z_0^{(2)}(\chi) = \lambda_0'\chi + (\lambda_0'' + 2\dot{\lambda}_0'\lambda_0')\chi^2/2$ yielding

$$\langle I\rangle = \lambda_0' = \mathrm{Tr}_{\mathrm{sys}}\mathcal{W}'\hat{\rho}^{\mathrm{stat}} \tag{4.6a}$$

and

$$\langle\langle I^2\rangle\rangle = \lambda_0'' + 2\dot{\lambda}_0'\lambda_0' = \mathrm{Tr}_{\mathrm{sys}}[\mathcal{W}'' - 2\mathcal{W}'\mathcal{R}\mathcal{W}']\hat{\rho}^{\mathrm{stat}} + 2\langle I\rangle \mathrm{Tr}_{\mathrm{sys}}[\dot{\mathcal{W}}' - \mathcal{W}'\mathcal{R}\dot{\mathcal{W}}]\hat{\rho}^{\mathrm{stat}}\ , \tag{4.6b}$$

with prime/dot denoting the χ/z-derivatives at zero and $\hat{\rho}^{\mathrm{stat}}$ ($\mathcal{R}$) being the stationary state (pseudoinverse) of the effective Liouvillean $\mathcal{L} \equiv \mathcal{W}(\chi=0;z=0)$ analogously to the previous chapter. The second term on the right hand side of (4.6b) constitutes the non-Markovian correction to the noise due to memory effects.

Now, we can apply these results to the case of a resonant level in the Fermi-edge-singularity (FES) regime, which exhibits strong memory effects as was shown theoretically [P.16] and

[2]The initial-condition term $\eta(\chi;t)$ does not contribute to the long-time FCS behavior, cf. P.6.

successfully compared to the experiment [P.15]. Following the experimental setup with the FES occurring at the resonance with the left lead ([53] and P.15) the Hamiltonian (2.1) is supplemented by the interaction term $H_{\rm int} = d^\dagger d \sum_{k_L,k'_L} V_{k_L k'_L} c^\dagger_{k_L} c_{k'_L}$ describing the scattering of the left-lead electrons by the occupied resonant level. This interaction term is responsible for the Fermi-edge singularity and the resulting scattering phase shifts determine the FES critical exponent α [54]. The Coulomb interaction of the level with the right lead does not seem to play any role in the experiment. On the other hand, the tunnel couplings to the leads are dominated by the right one being much larger than the left $\gamma_R \gg \gamma_L$. The resonance is achieved by strongly biasing the right lead $\mu_R \to -\infty$ until the electrostatically gated resonant level hits the left-lead chemical potential. Under these circumstances it is possible to integrate out the right lead exactly while the left one can be treated in the lowest-order in the small γ_L. The GME for generalized occupations $\tilde{P}_i(\chi;t) \equiv \tilde{\rho}_{ii}(\chi;t)$, $i = 0, 1$ was derived by a physically-motivated decoupling for reduced-density matrix coherences $\tilde{\rho}_{01}(\chi;t)$, $\tilde{\rho}_{10}(\chi;t)$ in Ref. P.16 resulting in the generalized memory kernel

$$\mathbf{W}(\chi_L,\chi_R;z) = \begin{pmatrix} -\gamma_L(z) & \gamma_L^b(z)e^{-i\chi_L} + \gamma_R e^{i\chi_R} \\ \gamma_L(z)e^{i\chi_L} & -\gamma_L^b(z) - \gamma_R \end{pmatrix}, \tag{4.7}$$

with the counting fields $\chi_{L,R}$ at the left/right tunnel junction and the forward/backward non-Markovian tunneling rates given by

$$\begin{aligned} \gamma_L(z;\Delta) &\propto \Im\left[\left(\frac{i}{2\pi T}\right)^\alpha B\left(\frac{1-\alpha}{2} + \frac{z + \frac{\gamma_R}{2}(1-i\Delta)}{2\pi T}, \alpha\right)\right], \\ \gamma_L^b(z;\Delta) &= \gamma_L(z;-\Delta), \end{aligned} \tag{4.8}$$

with $\Delta \equiv 2(\mu_L - \epsilon_0)/\gamma_R$ the dimensionless energy distance from the resonant edge, α the FES exponent, and $B(x,y)$ the Beta function. When Eqs. (4.6a) and (4.6b) are applied to the kernel (4.7) we get regardless of the used counting field (which is the consequence of a charge conserving approximation) for the mean current and noise expressed in terms of the Fano factor the following expressions

$$I(\Delta) = e\frac{\gamma_R\gamma_L(0;\Delta)}{\gamma_R + \gamma_L(0;\Delta) + \gamma_L^b(0;\Delta)} \tag{4.9a}$$

and

$$\begin{aligned} F(\Delta) = 1 &- \frac{2\gamma_R\gamma_L(0;\Delta)}{(\gamma_R + \gamma_L(0;\Delta) + \gamma_L^b(0;\Delta))^2} \\ &+ 2\gamma_R\frac{(\gamma_R + \gamma_L^b(0;\Delta))\gamma_L'(0;\Delta) - \gamma_L^{b\prime}(0;\Delta)\gamma_L(0;\Delta)}{(\gamma_R + \gamma_L(0;\Delta) + \gamma_L^b(0;\Delta))^2}. \end{aligned} \tag{4.9b}$$

The second line of (4.9b) is the non-Markovian correction due to the memory effects. It should be mentioned that the mean current does not contain any non-Markovian correction in accordance with findings of Refs. [48], P.6, and P.11. In the shot noise limit $\Delta \gg 1$ both the backflow rate $\gamma_L^b(0;\Delta)$ as well as the non-Markovian corrections, i.e., the derivative terms in the second line of Eq. (4.9b) are negligible and we recover the standard Markovian expressions from Sec. 2.1. However, for low enough temperature $T \lesssim \gamma_R$ and close enough to the edge $|\Delta| \lesssim 10$ the non-Markovian corrections are relevant and their features are clearly visible in the Fano

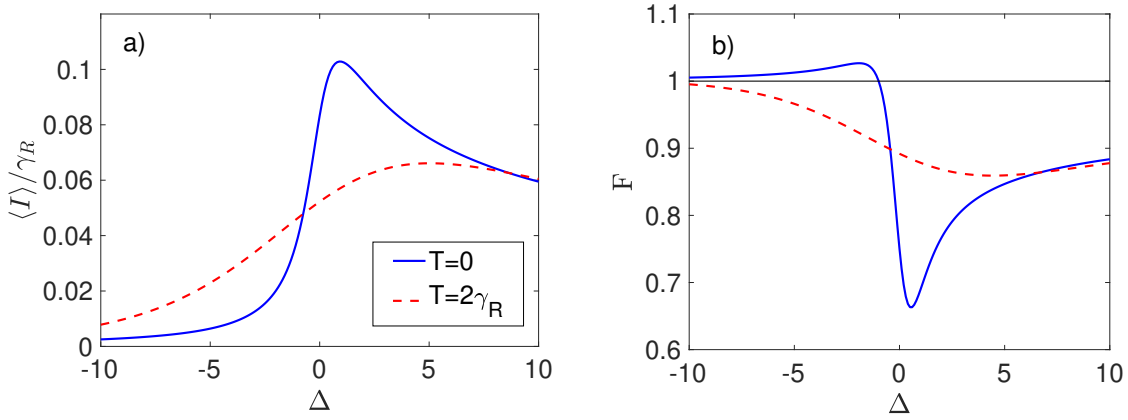

Figure 4: Current and noise in the Fermi-edge-singularity transport with the critical exponent $\alpha = 0.4$. a) Mean current and b) Fano factor as functions of dimensionless energy distance from the resonant edge $\Delta = 2(\mu_L - \epsilon_0)/\gamma_R$ for two different temperatures $T = 0$ (full blue line) and $T = 2\gamma_R$ (dashed red line). Poissonian limit $F = 1$ is depicted in b) by the thin horizontal line. [Reshaped figure taken from P.17.]

factor curves as depicted in Fig. 4 showing the mean current (4.9a) and Fano factor (4.9b) for two different temperatures as functions of the dimensionless distance from the edge Δ. We see at zero temperature the sharp FES peak in the mean current and accompanying strong suppression of the Fano factor above the edge and slightly super-Poissonian noise ($F > 1$) below it. These are effects associated with the strong quantum-induced memory which are destroyed by increased temperature as demonstrated by the other curve corresponding to $T = 2\gamma_R$. The crossover temperature is on the order of the dominant tunnel broadening $T \sim \gamma_R$. Straightforward generalization of the present calculation to the spinfull case with magnetic-field-induced Zeeman splitting and strong Coulomb blockade excluding level's double occupancy was successfully applied to the analysis of the experiment with excellent agreement with the measured data [P.15].

4.2 Nonequilibrium Green's function approach: inelastic effects in atomic wires (papers P.9, P.12, and P.13)

Complementarily to the previous case of GMEs based on expansion in the tunnel coupling with otherwise arbitrary interactions within the system there is an alternative route to the FCS evaluation starting from the noninteracting limit of electronic transport and incorporating many-body interactions perturbatively via the NEGF method [55]. There exists an extension of the standard NEGF scheme incorporating counting field(s) [56] based on the above-mentioned decorating of the Keldysh-Schwinger contour by the counting field and modifying the tunneling part of the Hamiltonian (4.2). The formal development of the theory is similarly to the standard NEGF method rather involved and lengthy, so I will only summarize the final conclusions and give operational description for the usage of the method. Readers interested in deeper levels

of the formalism are encouraged to consult relevant literature, in our context of resonant-level transport especially Refs. [56, 57].

The quantum formulation of the basic formula for the CGF at junction $\alpha = L, R$ reads [56, 57]

$$e^{S_\alpha(\chi_\alpha;t)} = \left\langle T_C \exp\left[-i\int_C d\tau H_{T\alpha}(\chi_\alpha(\tau);\tau)\right]\right\rangle \tag{4.10}$$

with the tunneling part of the Hamiltonian corresponding to the junction α modified according to the prescription with the counting field assuming different values on the two branches of the Keldysh-Schwinger contour C, more precisely $\chi_\alpha(\tau_-) = \chi_\alpha^-$ for $0 < \tau_- < t$ on the forward (or "$-$") branch and $\chi_\alpha(\tau_+) = \chi_\alpha^+$ for $0 < \tau_+ < t$ on the backward one ("$+$"), $\chi_\alpha(\tau) = 0$ otherwise. For long-enough t so that transients are negligible the CGF simplifies to $S_\alpha(\chi_\alpha; t \to \infty) = -it\mathcal{U}(\chi_\alpha^- = \chi_\alpha, \chi_\alpha^+ = -\chi_\alpha)$ [57] with the adiabatic potential which can be determined by

$$\frac{\partial \mathcal{U}(\chi_\alpha^-, \chi_\alpha^+)}{\partial \chi_\alpha^-} = \left\langle \frac{\partial H_{T\alpha}(\chi_\alpha(\tau);\tau)}{\partial \chi_\alpha^-}\right\rangle_{\chi_\alpha}. \tag{4.11}$$

The mean value is taken here with respect to the state determined by the modified Hamiltonian. The adiabatic potential is an analogy of the thermodynamic potentials, e.g., free energy, in the equilibrium statistical physics. They can be evaluated directly by perturbative methods involving Feynman diagrams but when infinite resummations are needed, they cannot be done directly for the thermodynamic potentials. Rather, their derivatives for example with respect to coupling strength are used which effectively leads to evaluation of Green's functions. Perturbation expansions for Green's functions can be resummed straightforwardly [58]. Here, the situation is exactly analogous — the derivative of the adiabatic potential constitutes some kind of (nonequilibrium and generalized by the counting field) Green's function for which a perturbation theory in terms of Feynman diagrams can be formulated with the possibility of resummations, i.e., dressing the lines of diagrams. Moreover, the CGF itself is basically never needed, but its derivatives at least of the first order are, see above the prescriptions for the cumulants and large-deviation rate function. Thus, the derivative of the adiabatic potential is the most natural and needed quantity to calculate.

As already mentioned the derivative of the adiabatic potential is an equal-time Green's function involving both the resonant-level and lead operators and when the many-body interaction is localized on the resonant level only (as, for example, in the Anderson model with local Coulomb interaction U or for localized electron-vibration couplings studied here) it can be expressed in terms of the local interacting Green's functions only via a sort of a generalized Meir-Wingreen formula [59]. For the single resonant level with localized interaction this formula gives for the derivative of the CGF ([57] and P.9)

$$\lim_{t\to\infty}\frac{1}{t}\frac{\partial S_\alpha(\chi_\alpha;t)}{\partial(i\chi_\alpha)} = \int\frac{d\epsilon}{2\pi i}\gamma_\alpha(\epsilon)\left[e^{-i\chi_\alpha}(1-f_\alpha(\epsilon))G_{\chi_\alpha}^{-+}(\epsilon) + e^{i\chi_\alpha}f_\alpha(\epsilon)G_{\chi_\alpha}^{+-}(\epsilon)\right]. \tag{4.12}$$

Green's functions $G_{\chi_\alpha}^{\pm\mp}(\epsilon)$ are the appropriate Keldysh components in the energy domain of the generalized NEGF defined via $G_{\chi_\alpha}(\tau,\tau') \equiv -i\left\langle T_C d(\tau)d^\dagger(\tau')\right\rangle_{\chi_\alpha}$. The difference from the definition of standard NEGF is in the mean value being taken with respect to the modified tunneling Hamiltonian including the counting field χ_α. This has significant consequences for the properties of these generalized NEGFs — because of the presence of two opposite counting fields at the two branches of the Keldysh-Schwinger contour the fundamental identity connecting the

four components of standard NEGFs is broken, i.e., $G^{--}+G^{++}\neq G^{-+}+G^{+-}$. Consequently, the customary NEGF reduction to retarded, advanced, and Keldysh (or lesser) components of Green's function only cannot be carried out. Now, all the four Keldysh components of the NEGF are independent and the Keldysh or Langreth-Wilkins rules for the perturbation expansion do not hold any longer. One must retain the whole 2x2 matrix structure in the perturbation scheme for the extended NEGFs, but otherwise it works straightforwardly.

Similarly as for the standard Meir-Wingreen formula also Eq. (4.12), which reduces to the normal Meir-Wingreen form when $\chi_\alpha=0$, contains all the complexity of many-body physics via Green's functions $G^{\pm\mp}_{\chi_\alpha}(\epsilon)$ which include the effects of interactions as well as the counting field. They yield all the characteristics of the interacting electronic transport, but of course their evaluation is the core problem. Generally, they are determined by the Dyson equation (check marks above the letters denote matrices in the Keldysh space) $\check{G}_\chi=\check{g}_\chi+\check{g}_\chi\check{\Sigma}_\chi\check{G}_\chi$ with free (i.e., without many-body interaction) NEGF $\check{g}_\chi(\epsilon)$ reading [57]

$$\check{g}_\chi(\epsilon)=\begin{pmatrix}\epsilon-\epsilon_0-i\sum_\alpha\gamma_\alpha(f_\alpha-\frac{1}{2}) & i\sum_\alpha\gamma_\alpha f_\alpha e^{i\chi_\alpha}\\ -i\sum_\alpha\gamma_\alpha(1-f_\alpha)e^{-i\chi_\alpha} & -\epsilon+\epsilon_0-i\sum_\alpha\gamma_\alpha(f_\alpha-\frac{1}{2})\end{pmatrix}^{-1}. \tag{4.13}$$

If one inserts the appropriate components of this non-interacting Green's function into Eq. (4.12), one obtains (we assume counting at the right junction)

$$\begin{aligned}\lim_{t\to\infty}\frac{1}{t}\frac{\partial S_R(\chi_R;t)}{\partial(i\chi_R)}&=\int\frac{d\epsilon}{2\pi}\frac{\mathcal{T}(\epsilon)\left[f_L(1-f_R)e^{-i\chi_R}-f_R(1-f_L)e^{i\chi_R}\right]}{1+\mathcal{T}(\epsilon)\left[f_L(1-f_R)(e^{-i\chi_R}-1)+f_R(1-f_L)(e^{i\chi_R}-1)\right]}\\&=i\frac{\partial}{\partial\chi_R}\int\frac{d\epsilon}{2\pi}\log\left[1+\mathcal{T}(\epsilon)\left[f_L(1-f_R)(e^{-i\chi_R}-1)+f_R(1-f_L)(e^{i\chi_R}-1)\right]\right]\end{aligned} \tag{4.14}$$

recovering the Levitov formula [2] for a ballistic point contact characterized here by the Breit-Wigner transmission coefficient $\mathcal{T}(\epsilon)=\frac{\gamma_L\gamma_R}{(\epsilon-\epsilon_0)^2+(\gamma_L+\gamma_R)^2/4}$ for the resonant level. Relation of this fully coherent result to its sequential-tunneling limit (2.7a) is explained in Ref. [22]. Many-body interactions are incorporated via the self-energy $\check{\Sigma}_\chi$ entering the Dyson equation; as usually it can be found in practice only approximately by the perturbation theory.

In Refs. P.9, P.12, and P.13 we have used the above outlined theory for studying inelastic corrections to the ballistic transport across a (generally multilevel) nanosystem weakly locally coupled to a vibrational mode with frequency ω (see Sec. 2.2 for details of the setup and notation). Due to assumed weak electron-vibration interaction (dimensionless coupling in experimentally relevant setups is on the order of 0.01) we used the simplest bare perturbation theory directly for the NEGF $\check{G}_\chi(\epsilon)$ in the lowest, i.e, second order in the coupling, which involves just the Hartree and Fock diagrams. In P.9 we considered only the single-level case while in P.12 the method was extended to general multi-orbital systems which is suitable for the implementation in *ab initio* packages (our theory was indeed included by Dr. Thomas Frederiksen into the `INELASTICA` code [60]).The experimentally interesting quantity is the inelastic noise signal $\Delta^{(2)}_{\rm inel}\equiv\partial\langle\langle I^2\rangle\rangle/\partial V|_{V=\omega+}-\partial\langle\langle I^2\rangle\rangle/\partial V|_{V=\omega-}$ at the inelastic threshold $V=\omega$ which is the noise analogy of the inelastic conductance jump. Tedious but straightforward calculations in P.9 yield for this quantity at zero temperature (in practice condition $\omega\gg T$ is well satisfied) $\Delta^{(2)}_{\rm inel}\propto 8\mathcal{T}^2-8\mathcal{T}+1$ as a function of the elastic transmission coefficient at the equilibrium chemical potential of the leads $\mathcal{T}\equiv\mathcal{T}(\mu)$. This quantity is positive for both large ($\mathcal{T}\to 1$) and small ($\mathcal{T}\to 0$) transmissions and changes sign to negative at crossing values

$\mathcal{T}_\pm = (2 \pm \sqrt{2})/4 \doteq 0.85, 0.15$. However, measurement of inelastic noise in gold atomic wires [9] found the crossing at $\mathcal{T}_+ \doteq 0.96$ (transparencies below ~ 0.6 could not be achieved in the experiment so the value $\mathcal{T}_-$ remains unknown).

The above mentioned theoretical result for the crossing values was only derived for a single level model, which is certainly not appropriate for an atomic chain consisting of several (~ 5) atoms, but two works building on our multi-orbital theory P.12 basically repeated the conclusions from this simple picture. Analytical theory for single elastic channel systems relevant to atomic chains [61] confirmed the $\mathcal{T}_+ = (2 + \sqrt{2})/4 \doteq 0.85$ as the upper bound for *any* single-channel system. Also elaborate *ab initio* simulations [60] including several channels could not recover the experimentally found crossing value above this bound. All the calculations mentioned so far assumed perfectly equilibrated vibration mode. That may not be necessarily the case in experiments so that we also studied in P.13 the opposite case of fully externally undamped vibrational mode. That calculation is more challenging since the counting field "penetrates" into the vibrational dynamics and more sophisticated resummation methods are needed even in the weak-coupling situation to account for the correlations between charge transfer and vibronic dynamics. These cause highly nontrivial backaction effects on the noise and FCS of such non-equilibrated system, which make even qualitative changes (e.g., different large-voltage asymptotics of inelastic noise and higher cumulants) with respect to the vibronic equilibrium case. Among others, also the crossing values are changed (in particular $\mathcal{T}_+ \doteq 0.816$), but not in a way explaining the experiment. Even though a systematic study of multi-orbital systems with a non-equilibrated vibrational mode has not been performed yet (to the best of my knowledge), the chances that the vibronic nonequilibrium could be responsible for the measured anomalous crossing value seem rather low. Thus the discrepancy between the experiment and theory remains a mystery so far.[3] Our calculation P.13 contradicted the earlier results of Ref. [31], which motivated us to come up with a more heuristic and physically intuitive approach to this problem to obtain an independent check of our microscopic results and resolve the discrepancy. As an answer to that call we performed the classical calculation in the large voltage limit P.18 described in Sec. 2.2.

[3]My personal opinion is that the sharp energy dependence of elastic characteristics of the measured junction observed already in the conductance curve in Fig. 1 of Ref. [9] invalidates the assumptions of the lowest-order expansion approach adopted by us (and others) and, consequently, our results are not applicable to those experimental data. Unfortunately, there are no indications that a similar experiment could be soon repeated, which would allow the community to address these problems more systematically.

Chapter 5

Summary

In this text serving as introduction to the attached 18 papers on the theory of noise and FCS in interacting nanoscopic systems I have tried to give a brief overview of concepts, methods, problems and results presented in those papers. Here, it may be appropriate to single out several important results achieved:

- General scheme for the evaluation of arbitrarily high cumulants in non-Markovian systems described by the GME formalism.
- Theoretical formulation and experimental proof of the existence of memory effects in the (zero-frequency) current noise.
- Discovery and experimental confirmation of a universal oscillatory behavior of high-order current cumulants.
- Comprehensive theoretical predictions for inelastic noise signal in nanosystems with weak electron-vibration interaction based on an extended formalism of the NGF.
- Usage of the lowest three current cumulants for the identification and detailed analysis of bistable quantum dynamics.

There are numerous interesting open questions remaining, but the rapid general progress made in the theory of FCS over the first decades of this century has more recently stalled. The main reason for this situation is the lack of relevant experiments, which is, especially in the field of condensed matter, a fatal issue. The experiments on noise are generally hard, the conjunction with nanoscopic objects makes them even harder (yet not impossible). Higher cumulants turned out to be nearly impossible — fighting the central limit theorem in its regime of validity is really challenging and none of the existing experiments has convinced the community that this path is worth further pursuit. This may sound like a complete failure story but it is not totally so.

First, noise measurements do exist, even if they are rare, and their conceptual understanding is sufficient. The FCS approach to evaluation of just noise is still an innovative one and it enabled to circumvent several technical subtleties encountered by different more direct approaches. It's likely that experimental nanoscopic noise studies will eventually become more common and will fuel the corresponding theoretical efforts.

Second, the counting approach itself has a great potential for identification of microscopic transport mechanisms in various regimes of operation of nanoscopic setups. It can be simply used as an effective theoretical tool to decipher internal dynamics of nanosystems just from

the electronic transport characteristics, let it be experimentally measured (like the Fermi edge singularity data) or just numerically calculated (like in the shuttle case). In this respect the method is not limited by the lack of experimental data as it can be equally well utilized for understanding transport mechanisms in systems simulated by advanced numerical techniques (such as Quantum Monte Carlo or Langevin dynamics) serving as "numerical experiments".

It is in this context, where I still do work with the FCS methods (although for classical stochastic systems — noisy phase dynamics in nanoscopic Josephson junctions), which enable me to efficiently extract highly nontrivial characteristics of the system dynamics (such as switching or phase-slips rates) that are very hard to obtain otherwise. So despite of the general decline of the original context within nanoscopic quantum electronic transport, the things I have learnt remain useful in other directions of my research, which (apart from nice 18 papers) proves the value of the invested efforts and time into their study.

Bibliography

[1] L. S. Levitov and G. B. Lesovik. Charge-distribution in quantum shot-noise. *JETP Lett.*, 58(3):230, 1993.

[2] L. S. Levitov, H. Lee, and G. B. Lesovik. Electron counting statistics and coherent states of electric current. *J. Math. Phys.*, 37:4845, 1996.

[3] Marlan O. Scully and M. Suhail Zubairy. *Quantum Optics*. Cambridge University Press, 1997.

[4] Hugo Touchette. The large deviation approach to statistical mechanics. *Physics Reports*, 478(1-3):1, 2009.

[5] S. Gustavsson, R. Leturcq, B. Simovic, R. Schleser, T. Ihn, P. Studerus, K. Ensslin, D. C. Driscoll, and A. C. Gossard. Counting statistics of single-electron transport in a quantum dot. *Phys. Rev. Lett.*, 96:076605, 2006.

[6] S. Gustavsson, R. Leturcq, B. Simovic, R. Schleser, P. Studerus, T. Ihn, K. Ensslin, D. C. Driscoll, and A. C. Gossard. Counting statistics and super-Poissonian noise in a quantum dot: Time-resolved measurements of electron transport. *Phys. Rev. B*, 74:195305, 2006.

[7] S. Gustavsson, R. Leturcq, T. Ihn, K. Ensslin, M. Reinwald, and W. Wegscheider. Measurements of higher order noise correlations in a quantum dot with a finite bandwidth detector. *Phys. Rev. B*, 75:075314, 2007.

[8] T. Fujisawa, T. Hayashi, R. Tomita, and Y. Hirayama. Bidirectional counting of single electrons. *Science*, 312(5780):1634, 2006.

[9] Manohar Kumar, Rémi Avriller, Alfredo Levy Yeyati, and Jan M. van Ruitenbeek. Detection of Vibration-Mode Scattering in Electronic Shot Noise. *Phys. Rev. Lett.*, 108:146602, 2012.

[10] J. Tobiska and Yu. V. Nazarov. Josephson Junctions as Threshold Detectors for Full Counting Statistics. *Phys. Rev. Lett.*, 93:106801, 2004.

[11] J. P. Pekola. Josephson Junction as a Detector of Poissonian Charge Injection. *Phys. Rev. Lett.*, 93(20):206601, 2004.

[12] B. Huard, H. Pothier, N.O. Birge, D. Esteve, X. Waintal, and J. Ankerhold. Josephson junctions as detectors for non-Gaussian noise. *Annalen der Physik*, 16(10-11):736–750, 2007.

[13] A. V. Timofeev, M. Meschke, J. T. Peltonen, T. T. Heikkila, and J. P. Pekola. Wide-band detection of the third moment of shot noise by a hysteretic Josephson junction. *Phys Rev. Lett.*, 98:207001, 2007.

[14] Q. Le Masne, H. Pothier, Norman O. Birge, C. Urbina, and D. Esteve. Asymmetric Noise Probed with a Josephson Junction. *Phys. Rev. Lett.*, 102:067002, 2009.

[15] C. W. J. Beenakker, M. Kindermann, and Yu. V. Nazarov. Temperature-Dependent Third Cumulant of Tunneling Noise. *Phys. Rev. Lett.*, 90:176802, 2003.

[16] C. W. Gardiner. *Handbook of Stochastic Methods*. Springer, second edition, 1990.

[17] Roger Balian. *From Microphysics to Macrophysics: Methods and Applications of Statistical Physics.* Springer, 2006.

[18] D. S. Golubev, M. Marthaler, Y. Utsumi, and Gerd Schön. Statistics of voltage fluctuations in resistively shunted Josephson junctions. *Phys. Rev. B*, 81:184516, 2010.

[19] Martin Žonda, Wolfgang Belzig, and Tomáš Novotný. Voltage noise, multiple phase-slips, and switching rates in moderately damped Josephson junctions. *Phys. Rev. B*, 91:134305, 2015.

[20] M. Kindermann and S. Pilgram. Statistics of heat transfer in mesoscopic circuits. *Phys. Rev. B*, 69:155334, 2004.

[21] Keiji Saito and Abhishek Dhar. Fluctuation Theorem in Quantum Heat Conduction. *Phys. Rev. Lett.*, 99:180601, 2007.

[22] D. A. Bagrets and Y. V. Nazarov. Full counting statistics of charge transfer in Coulomb blockade systems. *Phys. Rev. B*, 67:085316, 2003.

[23] Jie Ren and N. A. Sinitsyn. Braid group and topological phase transitions in nonequilibrium stochastic dynamics. *Phys. Rev. E*, 87:050101, 2013.

[24] Ya. M. Blanter and M. Büttiker. Shot noise in mesoscopic conductors. *Physics Reports*, 336(1-2):1, 2000.

[25] Dania Kambly, Christian Flindt, and Markus Büttiker. Factorial cumulants reveal interactions in counting statistics. *Phys. Rev. B*, 83:075432, 2011.

[26] C. W. Gardiner and P. Zoller. *Quantum Noise*. Springer, second edition, 2000.

[27] N. G. van Kampen. *Stochastic Processes in Physics and Chemistry*. North Holland, Amsterdam, second edition, 1992.

[28] Magnus Paulsson, Thomas Frederiksen, and Mads Brandbyge. Modeling inelastic phonon scattering in atomic- and molecular-wire junctions. *Phys. Rev. B*, 72:201101, 2005.

[29] Thomas Frederiksen, Magnus Paulsson, Mads Brandbyge, and Antti-Pekka Jauho. Inelastic transport theory from first principles: Methodology and application to nanoscale devices. *Phys. Rev. B*, 75:205413, 2007.

[30] Y. Utsumi, O. Entin-Wohlman, A. Ueda, and A. Aharony. Full-counting statistics for molecular junctions: Fluctuation theorem and singularities. *Phys. Rev. B*, 87:115407, 2013.

[31] D. F. Urban, R. Avriller, and A. Levy Yeyati. Nonlinear effects of phonon fluctuations on transport through nanoscale junctions. *Phys. Rev. B*, 82(12):121414, Sep 2010.

[32] T. Novotný, A. Donarini, and A.-P. Jauho. Quantum shuttle in phase space. *Phys. Rev. Lett.*, 90:256801, 2003.

[33] H. Spohn. Kinetic equations from Hamiltonian dynamics: Markovian limits. *Rev. Mod. Phys.*, 52(3):569, 1980.

[34] S. A. Gurvitz and Ya. S. Prager. Microscopic derivation of rate equations for quantum transport. *Phys. Rev. B*, 53(23):15932–15943, 1996.

[35] T. H. Stoof and Yu. V. Nazarov. Time-dependent resonant tunneling via two discrete states. *Phys. Rev. B*, 53(3):1050, 1996.

[36] R. Aguado and T. Brandes. Shot noise spectrum of open dissipative quantum two-level systems. *Phys. Rev. Lett.*, 92:206601, 2004.

[37] D. K. C. MacDonald. Spontaneous fluctuations. *Rep. Prog. Phys.*, 12:56, 1948.

[38] D. Kohen, C. C. Marston, and D. J. Tannor. Phase space approach to theories of quantum dissipation. *J. Chem. Phys.*, 107(13):5236, 1997.

[39] Mark T Mitchison and Martin B Plenio. Non-additive dissipation in open quantum networks out of equilibrium. *New Journal of Physics*, 20:033005, 2018.

[40] Michael Ridley, Viveka N. Singh, Emanuel Gull, and Guy Cohen. Numerically exact full counting statistics of the nonequilibrium Anderson impurity model. *Phys. Rev. B*, 97:115109, 2018.

[41] Andrew N. Jordan and Eugene V. Sukhorukov. Transport statistics of bistable systems. *Phys. Rev. Lett.*, 93:260604, 2004.

[42] W. Belzig and Yu. V. Nazarov. Full Counting Statistics of Electron Transfer between Superconductors. *Phys. Rev. Lett.*, 87:197006, 2001.

[43] Yu. V. Nazarov, editor. *Quantum Noise in Mesoscopic Physics*. Springer, Berlin, 2003.

[44] L. S. Levitov. The statistical theory of mesoscopic noise. In Yu. V. Nazarov, editor, *Quantum Noise in Mesoscopic Physics*, Berlin, 2003. Springer.

[45] Alex Kamenev. *Field Theory of Non-Equilibrium Systems*. Cambridge University Press, 2011.

[46] Patrick P. Hofer and A. A. Clerk. Negative Full Counting Statistics Arise from Interference Effects. *Phys Rev. Lett.*, 116:013603, 2016.

[47] Y. Makhlin, G. Schön, and A. Shnirman. Quantum-state engineering with Josephson-junction devices. *Rev. Mod. Phys.*, 73:357, 2001.

[48] A. Braggio, J. König, and R. Fazio. Full counting statistics in strongly interacting systems: Non-markovian effects. *Phys. Rev. Lett.*, 96:026805, 2006.

[49] Herbert Schoeller and Gerd Schön. Mesoscopic quantum transport: Resonant tunneling in the presence of a strong Coulomb interaction. *Phys. Rev. B*, 50(24):18436, 1994.

[50] J. König, H. Schoeller, and G. Schön. Zero-bias anomalies and boson-assisted tunneling through quantum dots. *Phys. Rev. Lett.*, 76:1715, 1996.

[51] Jonas Nyvold Pedersen and Andreas Wacker. Tunneling through nanosystems: Combining broadening with many-particle states. *Phys. Rev. B*, 72:195330, 2005.

[52] O. Karlström, C. Emary, P. Zedler, J. N. Pedersen, C. Bergenfeldt, P. Samuelsson, T. Brandes, and A. Wacker. A diagrammatic description of the equations of motion, current and noise within the second-order von Neumann approach. *J. Phys. A: Math. Theor.*, 46(6):065301, 2013.

[53] N. Maire, F. Hohls, T. Lüdtke, K. Pierz, and R. J. Haug. Noise at a Fermi-edge singularity in self-assembled InAs quantum dots. *Phys. Rev. B*, 75:233304, 2007.

[54] K. A. Matveev and A. I. Larkin. Interaction-induced threshold singularities in tunneling via localized levels. *Phys. Rev. B*, 46(23):15337, 1992.

[55] Hartmut Haug and Antti-Pekka Jauho. *Quantum Kinetics in Transport and Optics of Semiconductors*. Springer, Berlin, second edition, 2008.

[56] L. S. Levitov and M. Reznikov. Counting statistics of tunneling current. *Phys. Rev. B*, 70:115305, 2004.

[57] A. O. Gogolin and A. Komnik. Towards full counting statistics for the Anderson impurity model. *Phys. Rev. B*, 73:195301, 2006.

[58] A. A. Abrikosov, L. P. Gorkov, and I. E. Dzyaloshinski. *Methods of Quantum Field Theory in Statistical Physics*. Dover, 1975.

[59] Yigal Meir and Ned S. Wingreen. Landauer formula for the current through an interacting electron region. *Phys. Rev. Lett.*, 68(16):2512, 1992.

[60] R. Avriller and T. Frederiksen. Inelastic shot noise characteristics of nanoscale junctions from first principles. *Phys. Rev. B*, 86:155411, 2012.

[61] Sejoong Kim. Inelastic current noise in nanoscale systems: Scattering theory analysis. *Phys. Rev. B*, 89:035413, 2014.

List of original papers

P.1 Shot Noise of a Quantum Shuttle

T. Novotný, A. Donarini, C. Flindt, and A.-P. Jauho, *Phys. Rev. Lett.* **92**, 248302 (2004). DOI: 10.1103/PhysRevLett.92.248302

P.2 Current noise in a vibrating quantum dot array

C. Flindt, **T. Novotný**, and A.-P. Jauho, *Phys. Rev. B* **70**, 205334 (2004). DOI: 10.1103/PhysRevB.70.205334

P.3 Full counting statistics of nano-electromechanical systems

C. Flindt, **T. Novotný**, and A.-P. Jauho, *Europhys. Lett.* **69**, 475 (2005). DOI: 10.1209/epl/i2004-10351-x

P.4 Current noise spectrum of a quantum shuttle

C. Flindt, **T. Novotný**, and A.-P. Jauho, *Physica E* **29**, 411 (2005). DOI: 10.1016/j.physe.2005.05.040

P.5 Simple models suffice for the single dot quantum shuttle

A. Donarini, **T. Novotný**, and A.-P. Jauho, *New Journal of Physics* **7**, 237 (2005). DOI: 10.1088/1367-2630/7/1/237

P.6 Counting Statistics of Non-Markovian Quantum Stochastic Processes

C. Flindt, **T. Novotný**, A. Braggio, M. Sassetti, and A.-P. Jauho, *Phys. Rev. Lett.* **100**, 150601 (2008). DOI: 10.1103/PhysRevLett.100.150601

P.7 Josephson Junctions as Threshold Detectors of the Full Counting Statistics: Open issues

T. Novotný, *J. Stat. Mech.* (2009) P01050. DOI: 10.1088/1742-5468/2009/01/P01050

P.8 Universal oscillations in counting statistics

C. Flindt, C. Fricke, F. Hohls, **T. Novotný**, K. Netočný, T. Brandes, and R. J. Haug, *Proc. Natl. Acad. Sci. USA* **106**, 10116 (2009). DOI: 10.1073/pnas.0901002106

P.9 Phonon-assisted current noise in molecular junctions

F. Haupt, **T. Novotný**, and W. Belzig, *Phys. Rev. Lett.* **103**, 136601 (2009).
DOI: 10.1103/PhysRevLett.103.136601

P.10 Charge conservation breaking within generalized master equation description of electronic transport through dissipative double quantum dots

J. Prachař and **T. Novotný**, *Physica E* **42**, 565 (2010). DOI: 10.1016/j.physe.2009.06.026

P.11 Counting statistics of transport through Coulomb blockade nanostructures: high-order cumulants and non-Markovian effects

C. Flindt, **T. Novotný,** A. Braggio, and A.-P. Jauho, *Phys. Rev. B* **82**, 155407 (2010).
DOI: 10.1103/PhysRevB.82.155407

P.12 Current noise in molecular junctions: effects of the electron-phonon interaction

F. Haupt, **T. Novotný**, and W. Belzig, *Phys. Rev. B* **82**, 165441 (2010).
DOI: 10.1103/PhysRevB.82.165441

P.13 Nonequilibrium phonon backaction on the current noise in atomic-sized junctions

T. Novotný, F. Haupt, and W. Belzig, *Phys. Rev. B* **84**, 113107 (2011).
DOI: 10.1103/PhysRevB.84.113107

P.14 Noise calculations within the second-order von Neumann approach

P. Zedler, C. Emary, T. Brandes, and **T. Novotný**, *Phys. Rev. B* **84**, 233303 (2011). DOI: 10.1103/PhysRevB.84.233303

P.15 Strong quantum memory at resonant Fermi edges revealed by shot noise

N. Ubbelohde, K. Roszak, F. Hohls, N. Maire, R. J. Haug, and **T. Novotný**, *Sci. Rep.* **2**, 374 (2012). DOI: 10.1038/srep00374

P.16 Non-Markovian effects at the Fermi-edge singularity in quantum dots

K. Roszak and **T. Novotný**, *Phys. Scr.* **T151**, 014053 (2012). DOI: 10.1088/0031-8949/2012/T151/014053

P.17 Full counting statistics of electronic transport through interacting nanosystems

T. Novotný, *J. Comput. Electron.* **12**(3), 375 (2013). DOI: 10.1007/s10825-013-0475-6

P.18 Large-voltage behavior of charge transport characteristics in nanosystems with weak electron–vibration coupling

T. Novotný and W. Belzig, *Beilstein J. Nanotechnol.* **6**, 1853 (2015). DOI: 10.3762/bjnano.6.188